


Simultaneous metal–half-metal and spin transition in SrCoO₃ under compression

Han Hsu* and Sheng-Chieh Huang

Department of Physics, National Central University, Taoyuan City 32001, Taiwan

 (Received 7 March 2018; revised manuscript received 24 August 2018; published 6 November 2018)

In experiments, strontium cobaltite (SrCoO₃) has been confirmed to be a ferromagnetic metal (Curie temperature $T_C \approx 305$ K) at ambient conditions and remains in cubic perovskite structure up to ~ 60 GPa. Using local density approximation + self-consistent Hubbard U (LDA+ U_{sc}) calculations, we show that ferromagnetic metallic SrCoO₃ at low pressure is in an intermediate-spin (IS) state with $d^6\bar{L}$ character: nearly trivalent (Co³⁺) instead of tetravalent cobalt (Co⁴⁺) accompanied by spin-down O-2 p electron holes (ligand holes \bar{L}). Our calculations further predict that upon compression ($\gtrsim 7$ GPa), SrCoO₃ undergoes a transition to a low-spin (LS) ferromagnetic *half-metal* with an energy gap opened in the spin-up channel. Compared to the metallic IS state, the half-metallic LS state exhibits even more prominent $d^6\bar{L}$ character, including nearly nonmagnetic Co³⁺ and exceptionally large oxygen magnetic moments, which contribute most of the magnetization. By analyzing x-ray diffraction data of compressed single-crystal SrCoO₃, we point out an anomalous volume reduction of $\sim 1\%$. This previously unnoticed volume anomaly is in great agreement with our predictive calculations, providing quantitative evidence for the simultaneous metal–half-metal and spin transition in SrCoO₃.

DOI: [10.1103/PhysRevMaterials.2.111401](https://doi.org/10.1103/PhysRevMaterials.2.111401)

Since de Groot *et al.* predicted half-metals in 1983 [1], this class of materials has attracted great attention due to their unique electronic structures: nonzero density of states (DOS) at the Fermi level (E_F) in one spin channel and an energy gap opened in the other [2]. Behaving as a metal and an insulator simultaneously in one single material's different spin channels, half-metals have been considered as prominent spintronic materials. While the number of intrinsic half-metals are unknown, half-metallicity has been observed in materials of diverse types, including Heusler alloys [2–4], transition-metal oxides with spinel [5] or double perovskite structure [6–10], and heavy alkali-metal oxides [11]. Half-metallicity can also be induced by pressure; a few examples include double perovskites La₂CoMnO₆, La₂VMnO₆, and Sr₂NiReO₆ [12–14], and layered cobaltite Sr₂CoO₃F [15]. In this Rapid Communication, we report our predictive calculations of the simultaneous metal–half-metal and spin transition in cubic perovskite strontium cobaltite (SrCoO₃) under compression, and report our analysis of previous experiments to support this theoretical prediction. In a broader sense, a comprehensive study of compressed SrCoO₃ can also expand our knowledge of perovskite cobaltites (La_{1-x}Sr_x)CoO₃ ($0 \leq x \leq 1$), a family of materials being intensively studied for their complicated magnetic properties [16].

The complexity of (La_{1-x}Sr_x)CoO₃ largely arises from cobalt's multiple oxidation (Co³⁺ and Co⁴⁺) and spin states. Despite decades of effort, spin transitions in the end members LaCoO₃ and SrCoO₃ still remain controversial. At low temperatures ($T \lesssim 30$ K), LaCoO₃ is a nonmagnetic (NM) insulator with Co³⁺ in the low-spin (LS) state (total electron spin $S = 0$). Starting at ~ 30 K, LaCoO₃ undergoes a thermally induced spin transition into a paramagnetic insulator at ~ 90 K.

Both intermediate-spin (IS) and high-spin (HS) Co³⁺ have been suggested to explain the spin transition and the following paramagnetic phase, but a consensus has not been reached [17–44]. In addition to temperature, epitaxial strain can also induce spin transition in LaCoO₃. In contrast to the NM bulk at low T , tensile-strained LaCoO₃ thin film is a ferromagnetic insulator. Various scenarios have been suggested, including IS Co³⁺ or a mixture of HS/LS Co³⁺ stabilized via expanded CoO₆ octahedra, oxygen vacancies, or superstructures in the thin film. The source of this ferromagnetism, however, still remains unclear [45–69].

In contrast to LaCoO₃, SrCoO₃ is a ferromagnetic (FM) metal with cubic perovskite structure ($Pm\bar{3}m$ symmetry) at ambient conditions [70,71]. SrCoO₃ was first suggested to have LS Co⁴⁺ ($t_{2g}^5 e_g^0$, $S = 1/2$) [72,73], but later theoretical and experimental works inclined to higher spin states [74–77]. Since the successful synthesis of single-crystal SrCoO₃, this material has attracted increasing attention due to its high Curie temperature ($T_C \approx 305$ K) and high magnetization ($M \approx 2.50\mu_B/f.u.$) [70,71]. Strain-induced magnetic and metal-insulator transitions in SrCoO₃ thin films have been reported [78–80], and properties and potential applications of SrCoO_{3- δ} ($0 \leq \delta \leq 0.5$) have also been investigated [81–85]. With magnetic cations in the octahedral site, SrCoO₃ is subject to spin or magnetic transitions upon compression. Relevant studies, however, have been scarce. To our knowledge, there are still no published spectroscopic studies of compressed SrCoO₃. So far, magnetic and transport measurements up to 1.28 GPa and neutron powder diffraction (NPD) up to 5.4 GPa have shown no signs of spin transition; single-crystal x-ray diffraction (XRD) at room temperature has shown SrCoO₃ remaining in $Pm\bar{3}m$ symmetry up to 60 GPa; furthermore, *no* signatures of CoO₆ octahedral tilt or distortion have been observed in low- T experiments down to 2 K, including NPD at 200 K [71]. It should be pointed out, however, that

*hanhsu@ncu.edu.tw

since both polycrystalline and single-crystal SrCoO₃ are synthesized at high- (P, T) conditions ($T > 1000$ K, $P \approx 6$ GPa) [70,82], the $Pm\bar{3}m$ phase may be a metastable phase at $T \leq 300$ K, despite its stability and robustness over a wide (P, T) range (0–60 GPa, from ≤ 200 to ~ 1000 K). Theoretical investigations for other possible structural phases (e.g., distorted perovskite [80]) and their stability with respect to brownmillerite SrCoO_{2.5} (a more favorable strontium cobaltite [70]) would be of interest, but not within the scope of our current goal to reveal potential novel properties of the robust $Pm\bar{3}m$ phase under compression.

In addition to materials research, spin transition is also of great importance in geoscience [86,87]. Major constituent minerals of the Earth's lower mantle (660–2390 km in depth, pressure range 23–135 GPa) contain 10–20 mol % of iron [86], which adopts various valence (Fe²⁺ or Fe³⁺) and spin states. As the pressure increases, iron in lower-mantle minerals undergoes a spin transition/crossover starting at $P \gtrsim 40$ GPa, drastically changing the host minerals' properties [88–118]. To investigate iron spin transition and its geophysical effects, tremendous efforts have been made. A major advance in theory is the development of the local density approximation + self-consistent Hubbard U (LDA+ U_{sc}) method, with the Hubbard U parameters computed from first principles self-consistently [119–122]. So far, LDA+ U_{sc} has successfully determined the HS-LS transition pressure and accompanying volume/elastic anomalies in several lower-mantle minerals, including bridgmanite (Fe-bearing MgSiO₃ perovskite) [114,115], ferropicrinite (Mg,Fe)O [116], ferromagnesite (Mg,Fe)CO₃ [117], and Fe-bearing new

hexagonal aluminous phase NaMg₂(Si, Al)₆O₁₂ [118]. Given its efficiency and accuracy, we adopt LDA+ U_{sc} in this work. For comparison, generalized-gradient approximation + Hubbard U (GGA+ U) calculations are also presented. Calculations in this work are performed using the QUANTUM ESPRESSO codes [123] with projected augmented wave pseudopotentials available at the Pslibrary website [124,125].

As mentioned above, the $Pm\bar{3}m$ phase of SrCoO₃ is the main focus of this work. In this phase, two distinct FM and one antiferromagnetic (AFM, G-type) states can be obtained in our calculation without applying any constraints; the NM state can be obtained by performing non-spin-polarized calculations. We compute self-consistent U_{sc} for SrCoO₃ in its ambient state (FM metal with lattice parameter $a = 3.8289$ Å [70]) and apply this U value to other magnetic states in the relevant pressure range. Within LDA, $U_{sc} = 7.5$ eV, which is in between a commonly chosen $U = 4.5$ and a computed $U = 10.8$ eV in the literature [76,81,85]. While the treatment of U_{sc} in this work is simpler than in Refs. [114–118], where the spin and/or volume dependences of U_{sc} were considered, the present simple treatment of U_{sc} still gives satisfactory results, as shall be shown below, and further discussed in the Supplemental Material [126]. Briefly speaking, LDA + U is derived from LDA + $U + J$ by neglecting the J term (which accounts for the exchange interactions), and the U parameters in LDA + U is the effective $U_{eff} \equiv U - J$. Within LDA+ U_{sc} , it is U_{eff} being computed self-consistently, not U or J alone [121–123]. Since J often increases with the total electron spin S , the self-consistent U_{eff} often decreases with S [114–118]. When adopting spin-dependent U_{eff} in LDA+ U

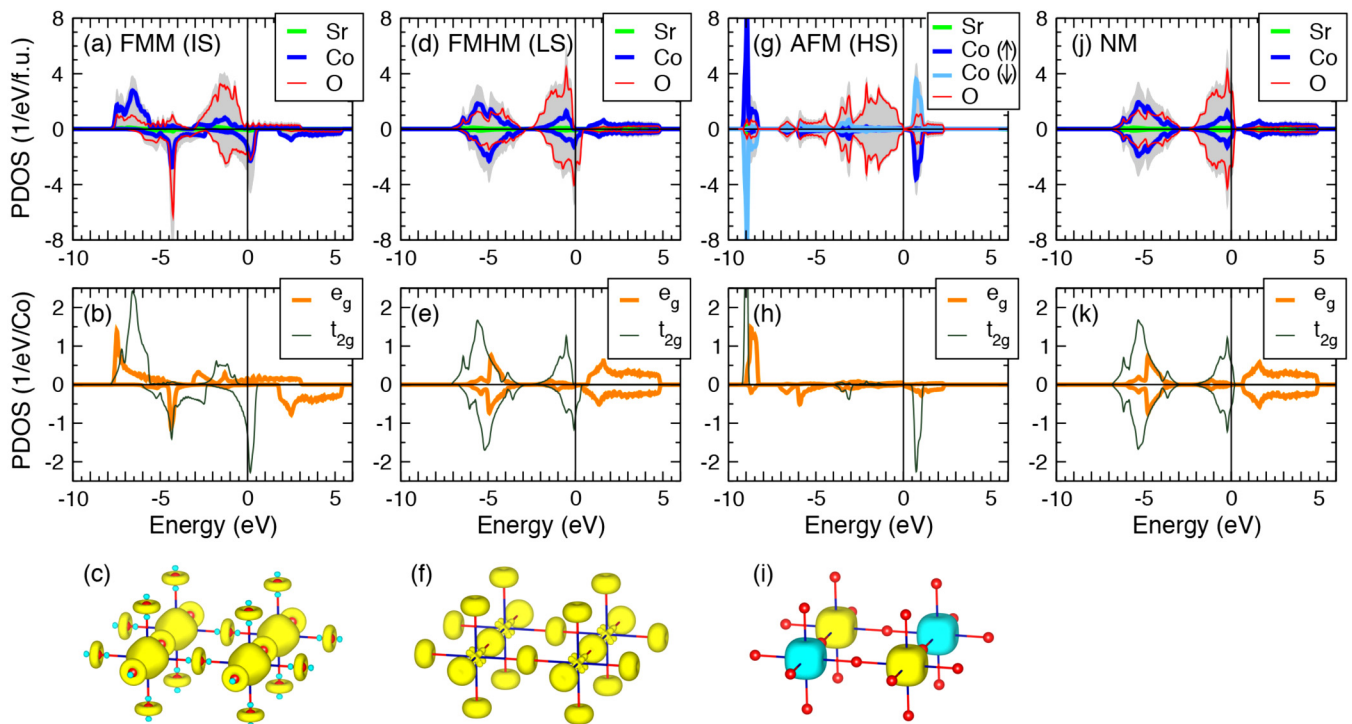


FIG. 1. DOS and electron spin density of SrCoO₃ in the (a)–(c) FMM (IS), (d)–(f) FMHM (LS), (g)–(i) AFM (HS), and (j), (k) NM states at their equilibrium volumes (see Table I). For each state, the total DOS (gray shade) and its projections onto each atomic species and Co-3d orbitals are plotted. The isosurface values of the electron spin density in panels (c), (f), and (i) are ± 0.03 a.u.⁻³ (yellow/cyan).

TABLE I. Equilibrium lattice parameter a_0 , relative energy ΔE with respect to the FMM (IS) state, total magnetization M , local magnetic moments μ_{Co} and μ_{O} , and Co-3d orbital occupancy of various magnetic states at zero pressure within LDA+ U_{sc} .

	ΔE (eV/f.u.)	a_0 (Å)	M (μ_{B} /f.u.)	μ_{Co} (μ_{B})	μ_{O} (μ_{B})	$t_{2g}^{(\uparrow)}$	$e_g^{(\uparrow)}$	$t_{2g}^{(\downarrow)}$	$e_g^{(\downarrow)}$
FMM (IS)	0	3.7521	2.36	1.823	0.162	2.994	1.564	2.193	0.550
FMHM (LS)	0.0283	3.7349	1.00	0.017	0.333	2.991	0.696	2.838	0.810
AFM (HS)	0.2451	3.8258	0.00	2.882	0.000	2.991	1.896	0.630	1.378
NM	0.0717	3.7349	0.00	0.000	0.000	2.925	0.742	2.925	0.742

without including the spin-dependent J term, a smaller U_{eff} for larger S sometimes leads to a significant underestimate of total energy for higher spin states. At the moment, however, computing J for each spin state is still highly challenging. To circumvent the energy underestimate for SrCoO₃ in higher spin states within LDA+ U , we only compute U_{eff} for ambient SrCoO₃ without considering its spin dependence [126].

Within LDA+ U_{sc} , the DOS and electron spin density of SrCoO₃ in all magnetic states at zero pressure are plotted in Fig. 1 (E_F aligned with 0 eV). Relevant parameters are listed in Table I, including the equilibrium lattice parameter (a_0), total magnetization (M), cobalt and oxygen magnetic moments (μ_{Co} and μ_{O}), and Co-3d orbital occupancy. For convenience, the total energy is expressed in terms of the relative energy (ΔE) with respect to the ferromagnetic metallic (FMM) state [Figs. 1(a)–1(c)]. As indicated in Table I, the FMM state is the ground state (lowest ΔE) with $M = 2.36\mu_{\text{B}}$ /f.u., in agreement with experiments [70,71]. Given its cobalt magnetic moment ($\mu_{\text{Co}} = 1.823\mu_{\text{B}}$) and orbital occupancy ($t_{2g}^{(\uparrow)} = 2.994$, $t_{2g}^{(\downarrow)} = 2.193$), the oxidation and spin state of Co in the FMM state is closer to IS Co³⁺ ($t_{2g}^5 e_g^1$, $S = 1$) rather than IS Co⁴⁺ ($t_{2g}^4 e_g^1$, $S = 3/2$) or HS Co³⁺ ($t_{2g}^4 e_g^2$, $S = 2$). The significant oxygen magnetic moment [$\mu_{\text{O}} = 0.162\mu_{\text{B}}$; see also Fig. 1(c)] is an indication of spin-down O-2p electron holes (ligand holes \bar{L}). A ferromagnetic ground state with $d^6\bar{L}$ character is consistent with x-ray absorption spectra [77] and previous theoretical studies [74–76], including dynamical mean-field theory (DMFT). Remarkable similarities between the LDA+ U_{sc} and DMFT results [76] include the shape of the DOS [Fig. 1(a)], orbital polarization at E_F (e_g in the spin-up and t_{2g} in the spin-down channel) [Fig. 1(b)], and negative spin polarization of the O-2p _{σ} orbital [cyan lobes in Fig. 1(c)].

The other FM state of SrCoO₃ [Figs. 1(d)–1(f)] has $M = 1.00\mu_{\text{B}}$ /f.u. and an energy gap ($E_g = 0.845$ eV) opened in the spin-up channel. This ferromagnetic *half-metallic* (FMHM) state exhibits even more prominent $d^6\bar{L}$ character. Co in this FMHM state is nearly nonmagnetic LS Co³⁺ ($t_{2g}^6 e_g^0$, $S = 0$), as indicated by its nearly vanishing Co magnetic moment ($\mu_{\text{Co}} = 0.017\mu_{\text{B}}$) and nearly completely filled Co- t_{2g} orbitals ($t_{2g}^{(\uparrow)} = 2.991$, $t_{2g}^{(\downarrow)} = 2.838$). The exceptionally large oxygen magnetic moment [$\mu_{\text{O}} = 0.333\mu_{\text{B}}$; see also Fig. 1(f)] indicates more ligand holes in this FMHM (LS) state than in the FMM (IS) state; it also indicates that oxygen contributes most of the magnetization in the FMHM (LS) state. Remarkably, the coexistence of a majority-spin gap and large oxygen magnetic moments is rare in transition-metal oxides but more common in heavy alkali-metal oxides [11]. To better view

the majority-spin gap, we also plot the band structures of the FMM (IS) and FMHM (LS) states in Fig. 2.

In contrast to the FMM (IS) and FMHM (LS) states, the AFM state of SrCoO₃ [Figs. 1(g)–1(i)] does not exhibit much $d^6\bar{L}$ character. Its large Co magnetic moment ($\mu_{\text{Co}} = 2.882\mu_{\text{B}}$) and nearly half-filled Co- t_{2g} orbitals ($t_{2g}^{(\uparrow)} = 2.991$, $t_{2g}^{(\downarrow)} = 0.630$) suggest HS Co⁴⁺ ($t_{2g}^3 e_g^2$, $S = 5/2$) with strong hybridization with O-2p electrons. Within LDA+ U_{sc} , the AFM (HS) state is not the ground state and has the largest equilibrium volume. This result suggests that AFM order can be observed in expanded or tensile-strained SrCoO₃, consistent with other calculations and experiments [78,79]. The DOS of the NM state is shown in Figs. 1(j) and 1(k).

The equations of state $E(V)$ and compression curves $V(P)$ of SrCoO₃ in all magnetic states within LDA+ U_{sc} ($U_{\text{sc}} = 7.5$ eV), GGA+ U_{sc} ($U_{\text{sc}} = 7.4$ eV), and GGA+ U (with a chosen $U = 5.4$ eV) are plotted in Fig. 3, where the computa-

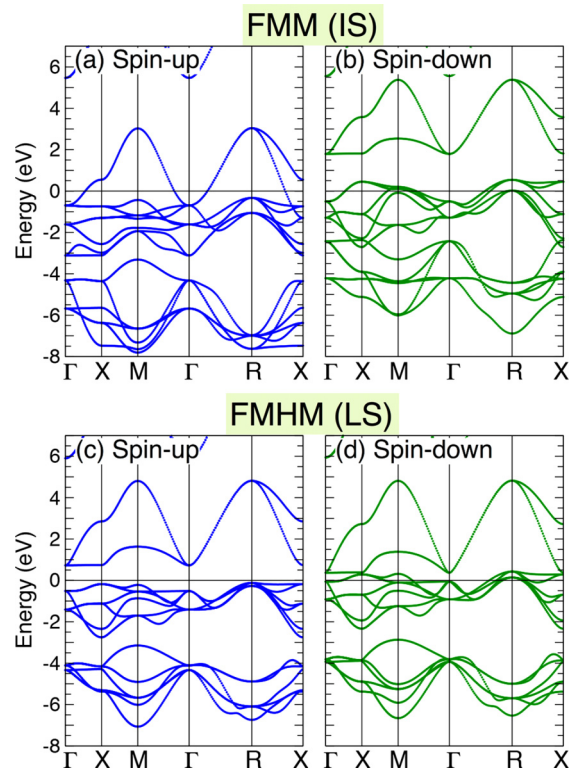


FIG. 2. Band structure of SrCoO₃ in the (a),(b) FMM (IS) and (c),(d) FMHM (LS) states at zero pressure within LDA+ U_{sc} . An energy gap of 0.845 eV is opened in the spin-up channel of the FMHM (LS) state, as shown in panel (c).

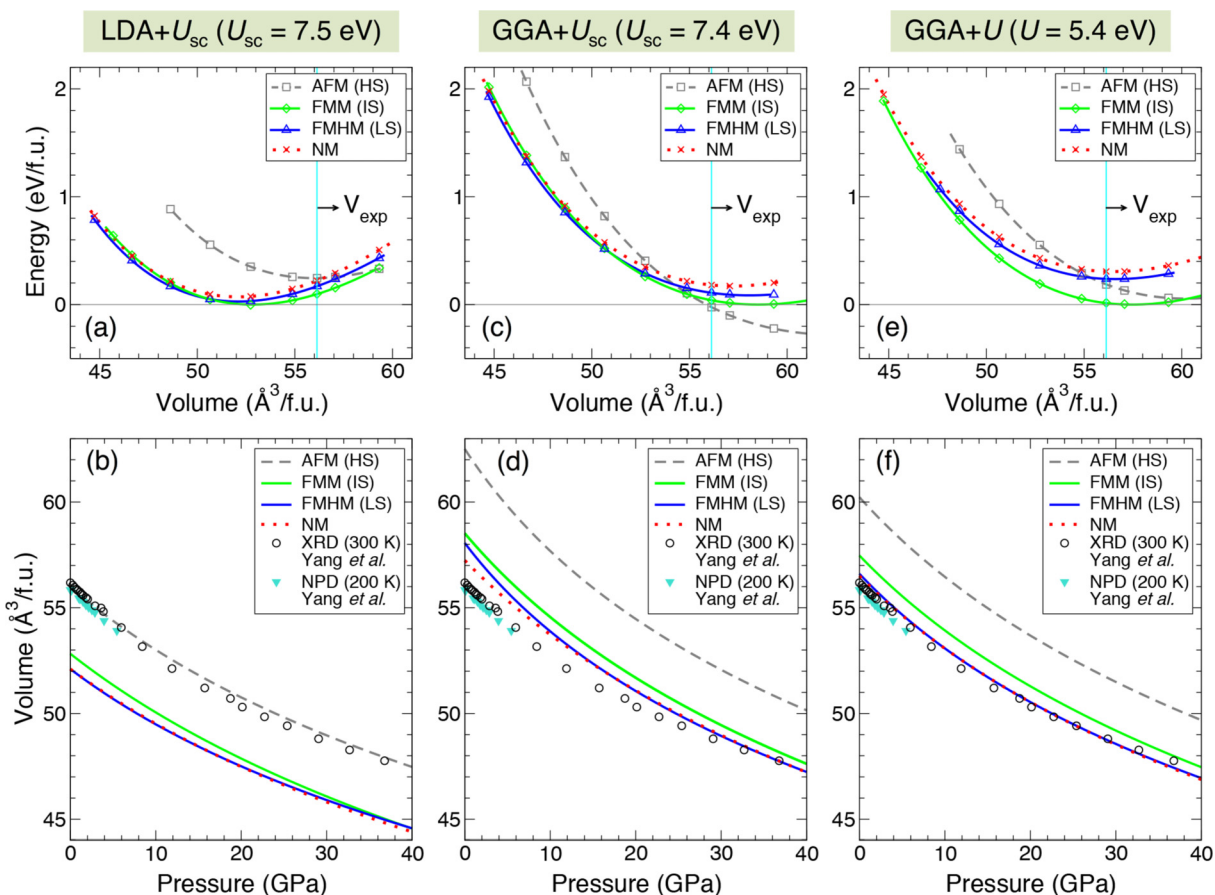


FIG. 3. The equations of state $E(V)$ and compression curves $V(P)$ of SrCoO_3 in the FMM (IS), FMHM (LS), AFM (HS), and NM states within (a),(b) $\text{LDA}+U_{\text{sc}}$, (c),(d) $\text{GGA}+U_{\text{sc}}$, and (e),(f) $\text{GGA}+U$. Notice that $\text{LDA}+U_{\text{sc}}$ correctly predicts the FMM (IS) state as the ground state at $P = 0$.

tion results are fitted with the third-order Birch-Murnaghan equation of state (3rd BM EoS). In each case, the energy reference is set at the equilibrium of the FMM (IS) state. Relevant parameters (ΔE , a_0 , and M) are listed in Table II, along with experimental results [70,71]. As shown in Fig. 3 and Table II, $\text{LDA}+U_{\text{sc}}$ correctly finds the FMM (IS) state as the ground state at $P = 0$, while $\text{GGA}+U_{\text{sc}}$ overly favors the AFM (HS) state. A possible reason is that the electron

delocalization in LDA is already corrected to some extent in GGA and may be overcompensated in $\text{GGA}+U$ with a large U , making $\text{GGA}+U_{\text{sc}}$ favor the AFM (HS) state (with more prominent electron localization and insulating characters) over the FMM (IS) state (with itinerant characters) at low pressure. By lowering the U parameter by 2 eV, $\text{GGA}+U$ with $U = 5.4$ eV no longer favors the AFM (HS) state. As to the structural parameters, both $\text{GGA}+U_{\text{sc}}$ and $\text{GGA}+U$

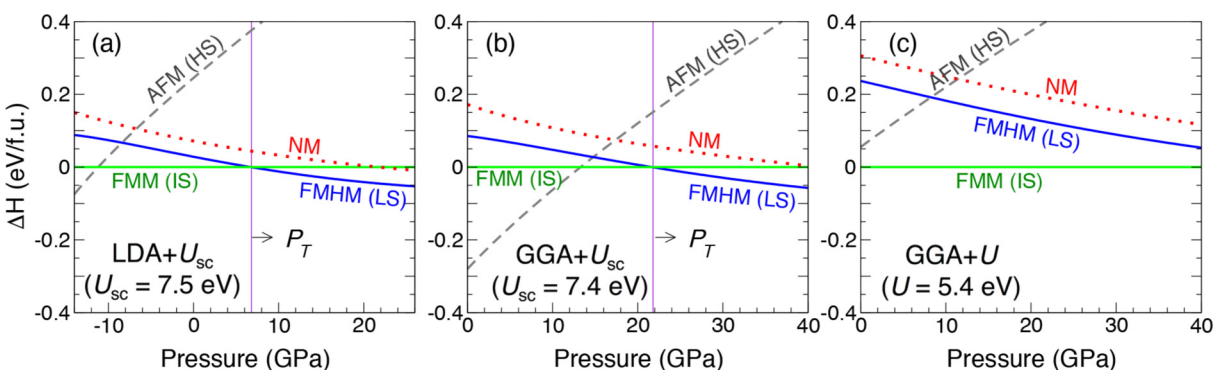


FIG. 4. Relative enthalpies (ΔH) of the FMHM (LS), AFM (HS), and NM states with respect to the FMM (IS) state within (a) $\text{LDA}+U_{\text{sc}}$, (b) $\text{GGA}+U_{\text{sc}}$, and (c) $\text{GGA}+U$. The IS-LS transition pressure (P_T) is indicated by the vertical purple lines.

TABLE II. ΔE , a_0 , and M (see definition in Table I) at zero pressure within LDA+ U_{sc} , GGA+ U_{sc} , and GGA+ U . Experimental data are also presented.

		ΔE (eV/f.u.)	a_0 (Å)	M (μ_B /f.u.)
Experiment at 300 K [70]		—	3.8289	2.50
Experiment at 200 K [71]		—	3.8227	1.76
LDA+ U_{sc} ($U_{sc} = 7.5$ eV)	FMM (IS)	0	3.7521	2.36
	FMHM (LS)	0.0283	3.7349	1.00
	AFM (HS)	0.2451	3.8258	0.00
	NM	0.0717	3.7349	0.00
GGA+ U_{sc} ($U_{sc} = 7.4$ eV)	FMM (IS)	0	3.8824	2.46
	FMHM (LS)	0.0854	3.8722	1.00
	AFM (HS)	-0.2801	3.9687	0.00
	NM	0.1720	3.8539	0.00
GGA+ U ($U = 5.4$ eV)	FMM (IS)	0	3.8591	2.70
	FMHM (LS)	0.2366	3.8397	1.00
	AFM (HS)	0.0552	3.9198	0.00
	NM	0.3060	3.8373	0.00

overestimate the equilibrium lattice parameter a_0 of the FMM (IS) state, while LDA+ U_{sc} underestimates a_0 by $\sim 2\%$. Regardless of the computation methods, the AFM (HS) state has significantly larger volume than the other three states, and the FMM (IS) is slightly larger than the FMHM (LS) and NM states by $\sim 1\%$, as can be observed in Figs. 3(b), 3(d), and 3(f).

To find out the most energetically favorable magnetic state of SrCoO₃ under compression, we plot the relative enthalpies ($\Delta H \equiv \Delta E + P\Delta V$) of all magnetic states with respect to the FMM (IS) state in Fig. 4. The results given by LDA+ U_{sc} , GGA+ U_{sc} , and GGA+ U are qualitatively similar: In the lowermost pressure range, the AFM (HS) state is the most favorable; as the pressure increases, the FMM (IS) state becomes the most favorable, followed by the FMHM (LS) state at $P > P_T$ (P_T is the IS-LS transition pressure, indicated by the vertical lines in Fig. 4). Within LDA+ U_{sc} [Fig. 4(a)], the FMM (IS) state is the most favorable in the region of $-11.2 < P < 6.8$ GPa. When expanded to $P < -11.2$ GPa, the AFM (HS) state is the most favorable; when compressed to $P > 6.8$ GPa, the FMHM (LS) state is the most favorable ($P_T = 6.8$ GPa). Within GGA+ U_{sc} [Fig. 4(b)] and GGA+ U [Fig. 4(c)], the FMM (IS) state is the most favorable in the region of $13.4 < P < 21.8$ and $-3.0 < P < 59.2$ GPa, with $P_T = 21.8$ and 59.2 GPa, respectively. Evidently, the GGA+ U results are highly sensitive to the choice of the Hubbard U . Likewise, varying U by 1–2 eV can drastically change the LDA+ U results (see Supplemental Material [126]). Comparing GGA+ U_{sc} and LDA+ U_{sc} , the main reason why GGA+ U_{sc} predicts a P_T much higher than LDA+ U_{sc} is that GGA tends to overestimate pressure and volume while LDA tends to underestimate these quantities, as shown in Figs. 3(b) and 3(d). Among all these methods, LDA+ U_{sc} predicts not only the correct FMM (IS) ground state at zero

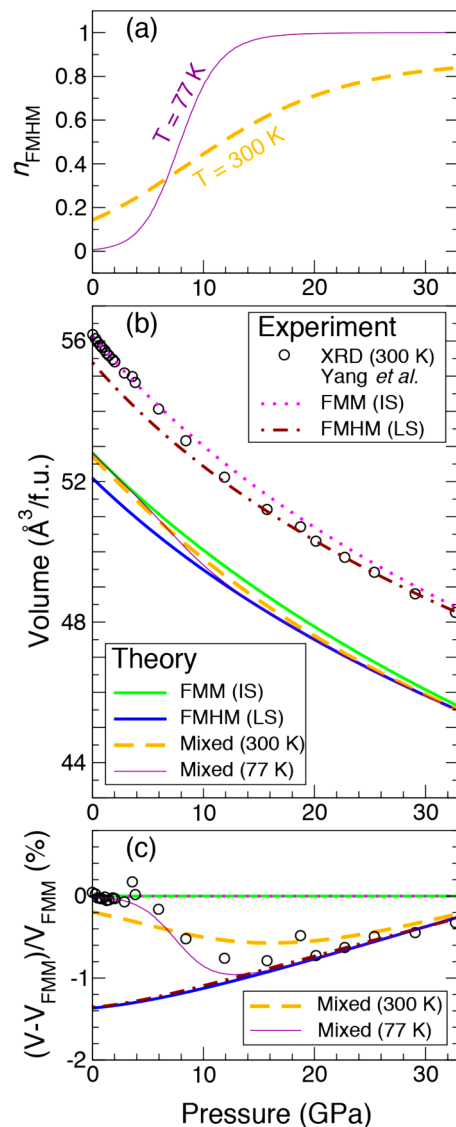


FIG. 5. Volume anomaly accompanying the simultaneous metal–half-metal and spin transition in SrCoO₃. (a) Fraction of the FMHM (LS) state, n_{FMHM} , in the mixed phase at $T = 300$ and 77 K within LDA+ U_{sc} ; (b) compression curves of the FMM (IS) and FMHM (LS) states and the mixed phase determined by theory and experiments [71]; (c) relative volume difference with respect to the FMM (IS) state determined by theory and experiments. See text and Supplemental Material [126] for further details about panels (b) and (c).

pressure but also the IS-LS transition pressure in great agreement with experiments, as discussed below.

While probing half-metallicity is challenging, signatures of pressure-induced spin transition are more easily detectable. A few examples include changes of x-ray emission and optical absorption spectra [88,89,92,93,113], and anomalous volume reduction upon compression, which arises from the significantly smaller cation size in the lower spin state [89,91,110,112,114,117,118]. Here we compare the computed volume anomaly with room-temperature XRD results. At $T \neq 0$, spin transition goes through a mixed phase consist-

ing of all possible states. Without the inclusion of vibrational free energy, the fraction n_i of state i ($i = \text{FMM}$, FMHM , or AFM) in the mixed phase can be determined using Eq. (1) with the constraint $\sum_i n_i = 1$, based on a thermodynamic model [91,104,106] detailed in the Supplemental Material [126],

$$\frac{n_i(P, T)}{n_{\text{FMM}}(P, T)} = \frac{2S_i + 1}{2S_{\text{FMM}} + 1} \exp\left(-\frac{\Delta H_i}{k_B T}\right), \quad (1)$$

where S_i is the total electron spin of the state i . The compression curve of the mixed phase (V_{mix}) is computed based on the assumption $V_{\text{mix}} = \sum_i n_i V_i$, where V_i is the compression curve of state i .

In Fig. 5(a), we plot the FMHM (LS) fraction n_{FMHM} within $\text{LDA}+U_{\text{sc}}$ for $T = 300$ and 77 K. In this (P, T) range, the AFM (HS) fraction is negligible ($n_{\text{AFM}} < 10^{-5}$); effectively, $n_{\text{FMM}} = 1 - n_{\text{FMHM}}$. At $T = 300$ K, the increase of n_{FMHM} is smoother than at 77 K. This temperature effect is a direct consequence of the $\exp(-\Delta H_i/k_B T)$ term in Eq. (1). In Fig. 5(b), we plot the mixed-phase compression curves V_{mix} for $T = 300$ (orange dashed line) and 77 K (purple thin line). Both curves undergo an anomalous volume reduction, deviating from V_{FMM} and merging into V_{FMHM} . At $T = 300$ and 77 K, the volume anomalies occur in the regions of $6 \lesssim P \lesssim 22$ and $6 \lesssim P \lesssim 12$ GPa, respectively, consistent with the increase of n_{FMHM} shown in Fig. 5(a). In experiments, the room-temperature XRD data in the pressure range 0–33 GPa [symbols in Fig. 5(b)] are of a mixed-phase compression curve; therefore, a single BM EoS would poorly fit these data points [71] (see also Supplemental Material [126]). We find that XRD data at $P < 7$ and $P > 20$ GPa can be fitted with two different 3rd BM EoS, indicated by the pink dotted ($V_0 = 56.159 \text{ \AA}^3$, $K_0 = 148.69$ GPa, $K'_0 = 5.34$) and brown dashed-dotted lines ($V_0 = 55.397 \text{ \AA}^3$, $K_0 = 151.31$ GPa, $K'_0 = 6.74$), which should be considered as the experimentally determined V_{FMM} and V_{FMHM} curves, respectively. In agreement with theory, the experimental V_{mix} (XRD data) undergoes an anomalous reduction, deviating from the experimental V_{FMM} and merging into V_{FMHM} . To better compare experiments and theory, we plot the relative volume difference with respect to the FMM (IS) state in Fig. 5(c), where the theoretical and

experimental V_{FMM} are used as the reference for the theoretical and experimental results, respectively (see also Supplemental Material [126]). Remarkably, the theoretically (blue solid) and experimentally (brown dashed-dotted) determined $(V_{\text{FMHM}} - V_{\text{FMM}})/V_{\text{FMM}}$ lines are in excellent agreement. On the other hand, the experimental $(V_{\text{mix}} - V_{\text{FMM}})/V_{\text{FMM}}$ (symbols) is in between the theoretical $T = 300$ (orange dashed) and 77 K (purple thin) lines, indicating that spin transition predicted by theory is smoother than observed in experiments. This slight difference, which also occurs in $(\text{Mg, Fe})\text{CO}_3$ [111,116], suggests that $|\Delta H|$ may be underestimated [see Eq. (1)]. We thus estimate that experiments performed at ~ 200 K would see a volume anomaly similar to the theoretical 77 K result; experiments performed at ~ 77 K would see an abrupt volume anomaly in the region of $6.5 \lesssim P \lesssim 8.5$ GPa (as long as SrCoO_3 remains in $Pm\bar{3}m$ symmetry at low T).

In summary, we have investigated cubic perovskite SrCoO_3 under compression using $\text{LDA}+U_{\text{sc}}$ calculations. Based on our calculations, SrCoO_3 at ambient pressure is a ferromagnetic metal in an intermediate-spin state with $d^6\bar{L}$ character, namely, nearly IS Co^{3+} ($t_{2g}^5 e_g^1$, $S = 1$) accompanied by spin-down O-2p electron holes. Upon compression ($\gtrsim 7$ GPa), SrCoO_3 undergoes a transition to a low-spin ferromagnetic half-metal with an energy gap opened in the spin-up channel. Compared to the metallic IS state, the half-metallic LS state exhibits even more prominent $d^6\bar{L}$ character, including nearly nonmagnetic LS Co^{3+} ($\mu_{\text{Co}} = 0.017\mu_B$), and exceptionally large oxygen magnetic moments ($\mu_{\text{O}} = 0.333\mu_B$), which contribute most of the magnetization. We have also analyzed room-temperature XRD data of compressed single-crystal SrCoO_3 and found an anomalous volume reduction ($\sim 1\%$) occurring in the pressure range 6–18 GPa. This previously unnoticed volume anomaly is in great agreement with our $\text{LDA}+U_{\text{sc}}$ calculations, providing quantitative evidence for the predicted metal–half-metal and spin transition. In short, our theoretical prediction points out potentially novel properties of SrCoO_3 for further investigation.

This work was supported by the Ministry of Science and Technology of Taiwan under Grants No. MOST 104-2112-M-008-005-MY3, No. 106-2119-M-001-028, No. 107-2112-M-008-022-MY3, and No. 107-2119-M-009-009-MY3.

-
- [1] R. A. de Groot, F. M. Mueller, P. G. van Engen, and K. H. J. Buschow, *Phys. Rev. Lett.* **50**, 2024 (1983).
- [2] M. I. Katsnelson, V. Yu. Irkhin, L. Chioncel, A. I. Lichtenstein, and R. A. de Groot, *Rev. Mod. Phys.* **80**, 315 (2008).
- [3] B. Balke, G. H. Fecher, H. C. Kandpal, C. Felser, K. Kobayashi, E. Ikenaga, J. J. Kim, and S. Ueda, *Phys. Rev. B* **74**, 104405 (2006).
- [4] R. Shan, H. Sukegawa, W. H. Wang, M. Kodzuka, T. Furubayashi, T. Ohkubo, S. Mitani, K. Inomata, and K. Hono, *Phys. Rev. Lett.* **102**, 246601 (2009).
- [5] Yu. S. Dedkov, U. Rudiger, and G. Guntherodt, *Phys. Rev. B* **65**, 064417 (2002).
- [6] Y. Tomioka, T. Okuda, Y. Okimoto, R. Kumai, K.-I. Kobayashi, and Y. Tokura, *Phys. Rev. B* **61**, 422 (2000).
- [7] H. Wu, *Phys. Rev. B* **64**, 125126 (2001).
- [8] H.-T. Jeng and G. Y. Guo, *Phys. Rev. B* **67**, 094438 (2003).
- [9] J. B. Philipp, P. Majewski, L. Alff, A. Erb, R. Gross, T. Graf, M. S. Brandt, J. Simon, T. Walther, W. Mader, D. Topwal, and D. D. Sarma, *Phys. Rev. B* **68**, 144431 (2003).
- [10] V. Pardo and W. E. Pickett, *Phys. Rev. B* **80**, 054415 (2009).
- [11] S. Naghavi, S. Chadov, C. Felser, G. H. Fecher, J. Kubler, K. Doll, and M. Jansen, *Phys. Rev. B* **85**, 205125 (2012).
- [12] S. Lv, X. Liu, H. Li, L. Han, Z. Wang, and J. Meng, *J. Comput. Chem.* **33**, 1433 (2012).
- [13] N. Zu, J. Wang, and Z. Wu, *J. Phys. Chem. C* **117**, 7231 (2013).
- [14] J. Wang, X. Sun, N. Zu, and Z. Wu, *J. Appl. Phys.* **114**, 163705 (2013).

- [15] X. Ou, F. Fan, Z. Li, H. Wang, and H. Wu, *Appl. Phys. Lett.* **108**, 092402 (2016).
- [16] B. Raveau and Md. M. Seikh, *Cobalt Oxides: From Crystal Chemistry to Physics* (Wiley-VCH, Weinheim, 2012).
- [17] M. A. Korotin, S. Yu. Ezhov, I. V. Solovyev, V. I. Anisimov, D. I. Khomskii, and G. A. Sawatzky, *Phys. Rev. B* **54**, 5309 (1996).
- [18] S. Yamaguchi, Y. Okimoto, and Y. Tokura, *Phys. Rev. B* **55**, R8666 (1997).
- [19] I. A. Nekrasov, S. V. Streltsov, M. A. Korotin, and V. I. Anisimov, *Phys. Rev. B* **68**, 235113 (2003).
- [20] K. Knížek, P. Novák, and Z. Jiráček, *Phys. Rev. B* **71**, 054420 (2005).
- [21] D. Phelan, D. Louca, S. Rosenkranz, S.-H. Lee, Y. Qiu, P. J. Chupas, R. Osborn, H. Zheng, J. F. Mitchell, J. R. D. Copley, J. L. Sarrao, and Y. Moritomo, *Phys. Rev. Lett.* **96**, 027201 (2006).
- [22] G. Vanko, J.-P. Rueff, A. Mattila, Z. Nemeth, and A. Shukla, *Phys. Rev. B* **73**, 024424 (2006).
- [23] R. F. Klie, J. C. Zheng, Y. Zhu, M. Varela, J. Wu, and C. Leighton, *Phys. Rev. Lett.* **99**, 047203 (2007).
- [24] T. Takami, J. S. Zhou, J. B. Goodenough, and H. Ikuta, *Phys. Rev. B* **76**, 144116 (2007).
- [25] M. M. Altarawneh, G.-W. Chern, N. Harrison, C. D. Batista, A. Uchida, M. Jaime, D. G. Rickel, S. A. Crooker, C. H. Mielke, J. B. Betts, J. F. Mitchell, and M. J. R. Hoch, *Phys. Rev. Lett.* **109**, 037201 (2012).
- [26] P. M. Raccah and J. B. Goodenough, *Phys. Rev.* **155**, 932 (1967).
- [27] S. Noguchi, S. Kawamata, K. Okuda, H. Nojiri, and M. Motokawa, *Phys. Rev. B* **66**, 094404 (2002).
- [28] Z. Ropka and R. J. Radwanski, *Phys. Rev. B* **67**, 172401 (2003).
- [29] K. Knizek, Z. Jirak, J. Hejtmanek, and P. Novak, *J. Phys.: Condens. Matter* **18**, 3285 (2006).
- [30] M. W. Haverkort, Z. Hu, J. C. Cezar, T. Burnus, H. Hartmann, M. Reuther, C. Zobel, T. Lorenz, A. Tanaka, N. B. Brookes, H. H. Hsieh, H.-J. Lin, C. T. Chen, and L. H. Tjeng, *Phys. Rev. Lett.* **97**, 176405 (2006).
- [31] A. Podlesnyak, S. Streule, J. Mesot, M. Medarde, E. Pomjakushina, K. Conder, A. Tanaka, M. W. Haverkort, and D. I. Khomskii, *Phys. Rev. Lett.* **97**, 247208 (2006).
- [32] H. Hsu, K. Umemoto, M. Cococcioni, and R. M. Wentzcovitch, *Phys. Rev. B* **79**, 125124 (2009).
- [33] K. Knizek, Z. Jirak, J. Hejtmanek, P. Novak, and W. Ku, *Phys. Rev. B* **79**, 014430 (2009).
- [34] Y. Jiang, F. Bridges, N. Sundaram, D. P. Belanger, I. E. Anderson, J. F. Mitchell, and H. Zheng, *Phys. Rev. B* **80**, 144423 (2009).
- [35] R. Eder, *Phys. Rev. B* **81**, 035101 (2010).
- [36] H. Hsu, P. Blaha, R. M. Wentzcovitch, and C. Leighton, *Phys. Rev. B* **82**, 100406(R) (2010).
- [37] V. Křápek, P. Novák, J. Kunes, D. Novoselov, D. M. Korotin, and V. I. Anisimov, *Phys. Rev. B* **86**, 195104 (2012).
- [38] G. Zhang, E. Gorelov, E. Koch, and E. Pavarini, *Phys. Rev. B* **86**, 184413 (2012).
- [39] S. Mukhopadhyay, M. W. Finnis, and N. M. Harrison, *Phys. Rev. B* **87**, 125132 (2013).
- [40] M. Karolak, M. Izquierdo, S. L. Molodtsov, and A. I. Lichtenstein, *Phys. Rev. Lett.* **115**, 046401 (2015).
- [41] J. Buckeridge, F. H. Taylor, and C. R. A. Catlow, *Phys. Rev. B* **93**, 155123 (2016).
- [42] K. Tomiyasu, J. Okamoto, H. Y. Huang, Z. Y. Chen, E. P. Sinaga, W. B. Wu, Y. Y. Chu, A. Singh, R.-P. Wang, F. M. F. de Groot, A. Chainani, S. Ishihara, C. T. Chen, and D. J. Huang, *Phys. Rev. Lett.* **119**, 196402 (2017).
- [43] Y. Shimizu, T. Takahashi, S. Yamada, A. Shimokata, T. Jin-no, and M. Itoh, *Phys. Rev. Lett.* **119**, 267203 (2017).
- [44] B. Chakrabarti, T. Birol, and K. Haule, *Phys. Rev. Mater.* **1**, 064403 (2017).
- [45] D. Fuchs, C. Pinta, T. Schwarz, P. Schweiss, P. Nagel, S. Schuppler, R. Schneider, M. Merz, G. Roth, and H. v. Lohneysen, *Phys. Rev. B* **75**, 144402 (2007).
- [46] D. Fuchs, E. Arac, C. Pinta, S. Schuppler, R. Schneider, and H. v. Lohneysen, *Phys. Rev. B* **77**, 014434 (2008).
- [47] J. W. Freeland, J. X. Ma, and J. Shi, *Appl. Phys. Lett.* **93**, 212501 (2008).
- [48] C. Pinta, D. Fuchs, M. Merz, M. Wissinger, E. Arac, H. v. Lohneysen, A. Samartsev, P. Nagel, and S. Schuppler, *Phys. Rev. B* **78**, 174402 (2008).
- [49] K. Gupta and P. Mahadevan, *Phys. Rev. B* **79**, 020406(R) (2009).
- [50] S. Park, P. Ryan, E. Karapetrova, J. W. Kim, J. X. Ma, J. Shi, J. W. Freeland, and W. Wu, *Appl. Phys. Lett.* **95**, 072508 (2009).
- [51] A. Herklotz, A. D. Rata, L. Schultz, and K. Dorr, *Phys. Rev. B* **79**, 092409 (2009).
- [52] V. V. Mehta, M. Liberati, F. J. Wong, R. V. Chopdekar, E. Arenholz, and Y. Suzuki, *J. Appl. Phys.* **105**, 07E503 (2009).
- [53] D. Fuchs, L. Dieterle, E. Arac, R. Eder, P. Adelman, V. Eyert, T. Kopp, R. Schneider, D. Gerthsen, and H. v. Lohneysen, *Phys. Rev. B* **79**, 024424 (2009).
- [54] J. M. Rondinelli and N. A. Spaldin, *Phys. Rev. B* **79**, 054409 (2009).
- [55] A. Posadas, M. Berg, H. Seo, A. de Lozanne, A. A. Demkov, D. J. Smith, A. P. Kirk, D. Zhernokletov, and R. M. Wallace, *Appl. Phys. Lett.* **98**, 053104 (2011).
- [56] G. E. Sterbinsky, P. J. Ryan, J.-W. Kim, E. Karapetrova, J. X. Ma, J. Shi, and J. C. Woicik, *Phys. Rev. B* **85**, 020403(R) (2012).
- [57] F. Rivadulla, Z. Bi, E. Bauer, B. Rivas-Murias, J. M. Vila-Funqueirino, and Q. Jia, *Chem. Mater.* **25**, 55 (2013).
- [58] L. Qiao, J. H. Jang, D. J. Singh, Z. Gai, H. Xiao, A. Mehta, R. K. Vasudevan, A. Tselev, Z. Feng, H. Zhou, S. Li, W. Prellier, X. Zu, Z. Liu, A. Borisevich, A. P. Baddorf, and M. D. Biegalski, *Nano Lett.* **15**, 4677 (2015).
- [59] M. Merz, P. Nagel, C. Pinta, A. Samartsev, H. v. Lohneysen, M. Wissinger, S. Uebe, A. Assmann, D. Fuchs, and S. Schuppler, *Phys. Rev. B* **82**, 174416 (2010).
- [60] H. Hsu, P. Blaha, and R. M. Wentzcovitch, *Phys. Rev. B* **85**, 140404(R) (2012).
- [61] H. Seo, A. Posadas, and A. A. Demkov, *Phys. Rev. B* **86**, 014430 (2012).
- [62] J. Bielecki, A. D. Rata, and L. Borjesson, *Phys. Rev. B* **89**, 035129 (2014).
- [63] W. S. Choi, J.-H. Kwon, H. Jeon, J. E. Hamann-Borrero, A. Radi, S. Macke, R. Sutarto, F. He, G. A. Sawatzky, V. Hinkov, M. Kim, and H. N. Lee, *Nano Lett.* **12**, 4966 (2012).
- [64] J. Fujioka, Y. Yamasaki, H. Nakao, R. Kumai, Y. Murakami, M. Nakamura, M. Kawasaki, and Y. Tokura, *Phys. Rev. Lett.* **111**, 027206 (2013).

- [65] J. Fujioka, Y. Yamasaki, A. Doi, H. Nakao, R. Kumai, Y. Murakami, M. Nakamura, M. Kawasaki, T. Arima, and Y. Tokura, *Phys. Rev. B* **92**, 195115 (2015).
- [66] A. Kushima, S. Yip, and B. Yildiz, *Phys. Rev. B* **82**, 115435 (2010).
- [67] N. Biskup, J. Salafranca, V. Mehta, M. P. Oxley, Y. Suzuki, S. J. Pennycook, S. T. Pantelides, and M. Varela, *Phys. Rev. Lett.* **112**, 087202 (2014).
- [68] V. V. Mehta, N. Biskup, C. Jenkins, E. Arenholz, M. Varela, and Y. Suzuki, *Phys. Rev. B* **91**, 144418 (2015).
- [69] A. O. Fumega and V. Pardo, *Phys. Rev. Mater.* **1**, 054403 (2017).
- [70] Y. Long, Y. Kaneko, S. Ishiwata, Y. Taguchi, and Y. Tokura, *J. Phys.: Condens. Matter* **23**, 245601 (2011).
- [71] J.-Y. Yang, C. Terakura, M. Medarde, J. S. White, D. Sheptyakov, X.-Z. Yan, N.-N. Li, W.-G. Yang, H.-L. Xia, J.-H. Dai, Y.-Y. Yin, Y.-Y. Jiao, J.-G. Cheng, Y.-L. Bu, Q.-F. Zhang, X.-D. Li, C.-Q. Jin, Y. Taguchi, Y. Tokura, and Y.-W. Long, *Phys. Rev. B* **92**, 195147 (2015).
- [72] T. Takeda and H. Watanabe, *J. Phys. Soc. Jpn.* **33**, 973 (1972).
- [73] H. Taguchi, M. Shimada, and M. Koizumi, *Mater. Res. Bull.* **13**, 1225 (1978).
- [74] R. H. Potze, G. A. Sawatzky, and M. Abbate, *Phys. Rev. B* **51**, 11501 (1995).
- [75] M. Zhuang, W. Zhang, A. Hu, and N. Ming, *Phys. Rev. B* **57**, 13655 (1998).
- [76] J. Kunes, V. Krapek, N. Parragh, G. Sangiovanni, A. Toschi, and A. V. Kozhevnikov, *Phys. Rev. Lett.* **109**, 117206 (2012).
- [77] M. Abbate, G. Zampieri, J. Okamoto, A. Fujimori, S. Kawasaki, and M. Takano, *Phys. Rev. B* **65**, 165120 (2002).
- [78] J. H. Lee and K. M. Rabe, *Phys. Rev. Lett.* **107**, 067601 (2011).
- [79] S. J. Callori, S. Hu, J. Bertinshaw, Z. J. Yue, S. Danilkin, X. L. Wang, V. Nagarajan, F. Klose, J. Seidel, and C. Ulrich, *Phys. Rev. B* **91**, 140405(R) (2015).
- [80] P. Rivero and C. Cazorla, *Phys. Chem. Chem. Phys.* **18**, 30686 (2016).
- [81] W. S. Choi, H. Jeon, J. H. Lee, S. S. Ambrose Seo, V. R. Cooper, K. M. Rabe, and H. N. Lee, *Phys. Rev. Lett.* **111**, 097401 (2013).
- [82] S. Balamurugan, K. Yamaura, A. B. Karki, D. P. Young, M. Arai, and E. Takayama-Muromachi, *Phys. Rev. B* **74**, 172406 (2006).
- [83] M. Hoffmann, V. S. Borisov, S. Ostanin, I. Mertig, W. Hergert, and A. Ernst, *Phys. Rev. B* **92**, 094427 (2015).
- [84] H. A. Tahini, X. Tan, U. Schwingenschlogl, and S. C. Smith, *ACS Catal.* **6**, 5565 (2016).
- [85] N. Lu, P. Zhang, Q. Zhang, R. Qiao, Q. He, H.-B. Li, Y. Wang, J. Guo, D. Zhang, Z. Duan, Z. Li, M. Wang, S. Yang, M. Yan, E. Arenholz, S. Zhou, W. Yang, L. Gu, C.-W. Nan, J. Wu, Y. Tokura, and P. Yu, *Nature (London)* **546**, 124 (2017).
- [86] J.-F. Lin, S. Speziale, Z. Mao, and H. Marquardt, *Rev. Geophys.* **51**, 244 (2013).
- [87] J. Badro, *Annu. Rev. Earth Planet Sci.* **42**, 231 (2014).
- [88] J. Badro, G. Fiquet, F. Guyot, J. Rueff, V. Struzhkin, G. Vanko, and G. Monaco, *Science* **300**, 789 (2003).
- [89] J.-F. Lin, V. V. Struzhkin, S. D. Jacobsen, M. Y. Hu, P. Chow, J. Kung, H. Liu, H.-k. Mao, and R. J. Hemley, *Nature (London)* **436**, 377 (2005).
- [90] S. Speziale, A. Milber, V. E. Lee, S. M. Clark, M. P. Pasternak, and R. Jeanloz, *Proc. Natl. Acad. Sci. USA* **102**, 17918 (2005).
- [91] T. Tsuchiya, R. M. Wentzcovitch, C. R. S. da Silva, and S. de Gironcoli, *Phys. Rev. Lett.* **96**, 198501 (2006).
- [92] A. F. Goncharov, V. V. Struzhkin, and S. D. Jacobsen, *Science* **312**, 1205 (2006).
- [93] J.-F. Lin, G. Vanko, S. D. Jacobsen, V. Iota, V. V. Struzhkin, V. B. Prakapenka, A. Kuznetsov, and C.-S. Yoo, *Science* **317**, 1740 (2007).
- [94] J. Crowhurst, J. M. Brown, A. F. Goncharov, and S. D. Jacobsen, *Science* **319**, 451 (2008).
- [95] R. M. Wentzcovitch, J. F. Justo, Z. Wu, C. R. S. da Silva, D. A. Yuen, and D. Kohlstedt, *Proc. Natl. Acad. Sci. USA* **106**, 8447 (2009).
- [96] H. Marquardt, S. Speziale, H. J. Reichmann, D. J. Frost, F. R. Schilling, and E. J. Garnero, *Science* **324**, 224 (2009).
- [97] D. Antonangeli, J. Siebert, C. M. Aracne, D. L. Farber, A. Bosak, M. Hoesch, M. Krisch, F. J. Ryerson, G. Fiquet, and J. Badro, *Science* **331**, 64 (2011).
- [98] Z. Wu, J. F. Justo, and R. M. Wentzcovitch, *Phys. Rev. Lett.* **110**, 228501 (2013).
- [99] E. Holmstrom and L. Stixrude, *Phys. Rev. Lett.* **114**, 117202 (2015).
- [100] Z. Wu and R. M. Wentzcovitch, *Proc. Natl. Acad. Sci. USA* **111**, 10468 (2014).
- [101] J. Badro, J. Rueff, G. Vanko, G. Monaco, G. Fiquet, and F. Guyot, *Science* **305**, 383 (2004).
- [102] J. Li, V. V. Struzhkin, H.-k. Mao, J. Shu, R. J. Hemley, Y. Fei, B. Mysen, P. Dera, V. Prakapenka, and G. Shen, *Proc. Natl. Acad. Sci. USA* **101**, 14027 (2004).
- [103] C. McCammon, I. Kantor, O. Narygina, J. Rouquette, U. Ponkratz, I. Sergueev, M. Mezouar, V. Prakapenka, and L. Dubrovinsky, *Nat. Geosci.* **1**, 684 (2008).
- [104] H. Hsu, K. Umemoto, Z. Wu, and R. M. Wentzcovitch, *Rev. Mineral Geochem.* **71**, 169 (2010).
- [105] H. Hsu, K. Umemoto, P. Blaha, and R. M. Wentzcovitch, *Earth Planet. Sci. Lett.* **294**, 19 (2010).
- [106] K. Umemoto, H. Hsu, and R. M. Wentzcovitch, *Phys. Earth Planet. In.* **180**, 209 (2010).
- [107] J.-F. Lin, H. Watson, G. Vanko, E. E. Alp, V. B. Prakapenka, P. Dera, V. Struzhkin, A. Kubo, J. Zhao, C. McCammon, and W. J. Evans, *Nat. Geosci.* **1**, 688 (2008).
- [108] Y. G. Yu, H. Hsu, M. Cococcioni, and R. M. Wentzcovitch, *Earth Planet. Sci. Lett.* **331-332**, 1 (2012).
- [109] R. M. Wentzcovitch, H. Hsu, and K. Umemoto, *Eur. J. Mineral.* **24**, 851 (2012).
- [110] B. Lavina, P. Dera, R. T. Downs, W. Yang, S. Sinogeikin, Y. Meng, G. Shen, and D. Schiferl, *Phys. Rev. B* **82**, 064110 (2010).
- [111] S. Fu, J. Yang, and J.-F. Lin, *Phys. Rev. Lett.* **118**, 036402 (2017).
- [112] Y. Wu, X. Wu, J.-F. Lin, C. A. McCammond, Y. Xiao, P. Chow, V. B. Prakapenka, T. Yoshino, S. Zhai, and S. Qin, *Earth Planet. Sci. Lett.* **434**, 91 (2016).
- [113] S. S. Lobanov, H. Hsu, J.-F. Lin, T. Yoshino, and A. F. Goncharov, *J. Geophys. Res. Solid Earth* **122**, 3565 (2017).
- [114] H. Hsu, P. Blaha, M. Cococcioni, and R. M. Wentzcovitch, *Phys. Rev. Lett.* **106**, 118501 (2011).

- [115] H. Hsu, Y. G. Yu, and R. M. Wentzcovitch, *Earth Planet. Sci. Lett.* **359**, 34 (2012).
- [116] H. Hsu and R. M. Wentzcovitch, *Phys. Rev. B* **90**, 195205 (2014).
- [117] H. Hsu and S. C. Huang, *Phys. Rev. B* **94**, 060404(R) (2016).
- [118] H. Hsu, *Phys. Rev. B* **95**, 020406(R) (2017).
- [119] M. Cococcioni and S. de Gironcoli, *Phys. Rev. B* **71**, 035105 (2005).
- [120] H. J. Kulik, M. Cococcioni, D. A. Scherlis, and N. Marzari, *Phys. Rev. Lett.* **97**, 103001 (2006).
- [121] B. Himmetoglu, R. M. Wentzcovitch, and M. Cococcioni, *Phys. Rev. B* **84**, 115108 (2011).
- [122] B. Himmetoglu, A. Floris, S. Gironcoli, and M. Cococcioni, *Int. J. Quantum Chem.* **114**, 14 (2014).
- [123] P. Giannozzi, O. Andreussi, T. Brumme, O. Bunau, M. Buongiorno Nardelli, M. Calandra, R. Car, C. Cavazzoni, D. Ceresoli, M. Cococcioni, N. Colonna, I. Carnimeo, A. Dal Corso, S. de Gironcoli, P. Delugas, R. A. DiStasio, Jr., A. Ferretti, A. Floris, G. Fratesi, G. Fugallo, R. Gebauer, U. Gerstmann, F. Giustino, T. Gorni, J. Jia, M. Kawamura, H.-Y. Ko, A. Kokalj, E. Kucukbenli, M. Lazzeri, M. Marsili, N. Marzari, F. Mauri, N. L. Nguyen, H.-V. Nguyen, A. Otero-de-la-Roza, L. Paulatto, S. Ponce, D. Rocca, R. Sabatini, B. Santra, M. Schlipf, A. P. Seitsonen, A. Smogunov, I. Timrov, T. Thonhauser, P. Umari, N. Vast, X. Wu, and S. Baroni, *J. Phys.: Condens. Matter* **29**, 465901 (2017).
- [124] See <https://dalcorso.github.io/pslibrary/>.
- [125] A. Dal Corso, *Comput. Mater. Sci.* **95**, 337 (2014).
- [126] See Supplemental Material at <http://link.aps.org/supplemental/10.1103/PhysRevMaterials.2.111401> about the computation of self-consistent U_{sc} , the effects of U on LDA+ U calculations, the thermodynamic model for the mixed phase, and our analysis to the XRD and NPD data in Ref. [71].